JOURNAL OF
Optical Communications
and Networking

Designing high-speed GEO-to-Moon optical wireless communication links

E. Ciaramella,* V. Spirito, and G. Cossu

Scuola Superiore Sant'Anna, Istituto TeCIP, Pisa, Italy
**e.ciaramella@sssup.it*

Received 3 October 2023; accepted 9 November 2023; published 21 December 2023

Moon exploration and colonization will strongly rely upon high-speed optical wireless communications over a huge distance (around 400,000 km). Here, we introduce a holistic model, including the propagation issues as well as the realistic communication limitations and the expected practical limitations. We focus on the communication issues in a link connecting a GEO satellite to a fixed Moon optical station: here, we consider the challenging 10 Gbit/s transmission rate, and we assume an optical pre-amplified receiver, which is today the only option for high speed; we then select three different modulation formats, with corresponding implementations and increasing complexity and performance. Under these assumptions, we estimate the common operating conditions at the forward error correction threshold and point out the role of the transmitter and receiver telescopes: for practical size (e.g., 1 m), relevant limitations arise, which we combine with the typical photons-per-bit sensitivity values in an optical link. We find that all considered modulation formats can be used at 10 Gbit/s, although with different margins and hardware requirements, particularly considering the size of the optical antennas. We then extend the analysis to higher rates, up to 40 Gbit/s. This work can open the way to the realization of optical wireless communication systems to/from the future Moon Village.

https://doi.org/10.1364/JOCN.507436

1. INTRODUCTION

Today we see a fast rising interest in the deep exploration of the Moon, leading to stable installments [1–5]. Various initiatives are being promoted by the USA, the EU, Canada, Japan, China, and India. As key non-limiting examples, the Moon Village concept envisions the deployment of robotic (first) and human (later) explorers [6], while Artemis I was recently launched [2]. Today, the lander of the Chandrayaan-3 mission is currently approaching the Moon [7].

However, it is widely recognized that, to reach these goals, we shall provide continuous high-speed data communication to the users on the Moon, likely through a Lunar Orbiting Platform-Gateway or a Lunar Ground Station. Among the supported applications, it should be considered that a single 8K-120 Hz camera would ask for hundreds of Mbit/s, if compressed (the uncompressed 8K format requires more than 20 Gbit/s) [8]. Other vital necessities may come from high-definition scanning for telemedicine, digital-twin applications, etc.

Therefore, for future-proof applications, high-speed wireless connectivity would target a minimum bit rate of 10 Gbit/s: this can be only achieved by using optical wireless communication (OWC) [9]. Indeed, the huge distance involves a beam spreading of electro-magnetic waves that is much lower in the optical region, thus strongly favoring optical against radio/microwave frequencies, especially at high bit rates [9–11]. Yet, optical links are not yet very common for space applications: the only real demonstration over interplanetary distances was the Lunar Laser Communication Demonstration (LLCD) by NASA in 2014, which demonstrated up to 622 Mbit/s downlink from the Moon surface to the Earth Optical Ground Station (OGS) using highly innovative optical technology and a photon-efficient modulation format: however, the link was not stable and had asymmetric capacity (uplink limited to a few tens of Mbit/s) [12].

It is worth recalling that, in any direct-to-Earth link, the Earth atmosphere determines a key limitation: in downlink, this can produce random fading on the optical received intensity; since optical loss is high, the fading can be often unmanageable [13–15]. The atmosphere has an even worse impact in uplink: this can result in much deeper fading. Therefore, a direct-to-Earth link could have the downlink randomly disappearing and the uplink very seriously limited in capacity. Hence, if we want to establish stable and reliable connections, those must require a two-hop link, i.e., using a GEO relay [16], as the one presented in Fig. 1. Unfortunately, a single GEO relay satellite would not provide 24 h connectivity to/from a fixed Moon station; however, it can be simply seen that at least two GEO satellites could be enough to provide a 100% reliable link to/from the Moon.

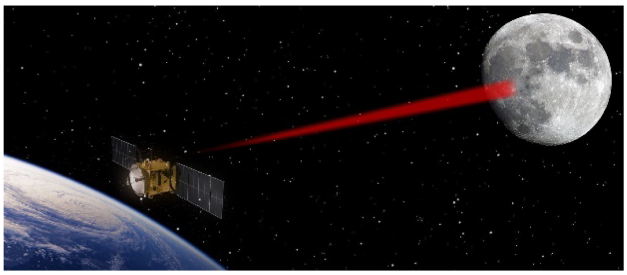

Fig. 1. Considered scenario: pictorial view of a GEO satellite communicating to the Moon by means of an optical signal.

In the Moon-to-GEO link, the attenuation would be mostly determined by the distance between the Moon Station and the GEO (around 400,000 km), thus practically constant. Loss would also be symmetric for both transmission directions: the propagation effects would be the same in both uplink and downlink and this would result in a link with similar design as in conventional fiber communications.

In order to realize this type of link in the required short time-frame, we should welcome that consolidated technologies could be used, as they need no special technological development. Indeed, our key assumption is to leverage upon the devices and techniques developed for fiber communications in the wavelength region of 1550 nm, which are the result of the huge R&D activity of the past 40 years [17].

This is possible only thanks to new types of OWC systems, which were recently introduced and are indicated as transparent systems [18,19]: indeed, they transparently combine the free-space path with existing fiber-based systems. This is achieved by optimized telescopes that, on one side, allow light to be transmitted from the transmitter fiber pigtail while, on the receiver side, they effectively couple the collected light into a single-mode fiber. Clearly, very precise optimization of the point alignment and tracking (PAT) is required, to make these systems work properly [20]. Various techniques able to achieve this goal were demonstrated in the past [21], and they were indeed successfully demonstrated in the LLCD experiments [12]. However, even for excellent PAT, the performance is affected by (minor) pointing errors, which are unavoidable and derive from different sources, including micro-vibrations of the telescopes. Pointing errors can be strongly reduced by various techniques, but typically remain on the order of 1 μrad.

In the following, we introduce a holistic approach to the optical communication design. We assume that an optimized PAT is implemented, and the telescope tracking is optimized to maintain a stable alignment during the communication, when the two extreme points move on their own orbits around Earth in free space. Then we study the communication system and combine the consolidated design methodology of optical fiber communications with the specific features of a long free-space optical link. We demonstrate that fiber-based components and techniques can be successfully exploited to achieve OWC Moon-to-GEO links at 10 Gbit/s.

The paper is structured as follows. In Section 2, we introduce the communication model and the technology that we are proposing to exploit: here, we first present the modeling assumption, then we motivate our choice of three alternative modulation formats and define their features in terms of photons-per-bit (PPB) sensitivities; finally, we present and discuss the impact of losses in the link budget. In Section 3, we then introduce symmetric and asymmetric link types, and thus provide the design of a Moon-to-GEO link at 10 Gbit/s, from a communication point of view. Finally, we evaluate the possibility of further upgrading these links to higher bit rates.

2. MODEL

A. Selected Modulation Formats and Their PPB Values

We highlight that in this type of OWC link, the transmission regime of the link is characterized by huge losses; the distance is the primary parameter determining these losses (assuming a stable alignment of the transmitter and receiver telescopes). In this case, the Moon-to-GEO distance depends on Earth–Moon distance, which is on average 385,000 km, and the exact position of the GEO, which has an almost circular orbit with 42,000 km radius (from the Earth's center). If we consider a specific GEO satellite, variations of free-space distance to a fixed point on the Moon should be calculated. However, considering direct visibility, we should restrict only to positions of the Moon and GEO on the same side of the rotation axis of the Earth; it can be easily seen that these variations of distance have a negligible impact on the total loss (around 0.5 dB). Therefore, in the following we assume the worst-case value (i.e., longest distance between Moon and GEO) is around 400,000 km. Actually, the distance can be a bit shorter because, mechanical constraints limit the field of regard of the telescope on the GEO, thus likely requiring three GEO satellites to provide a continuous connectivity. In this configuration, each GEO could be used for around 8 h/day.

It can be expected that the above losses can be partly balanced by means of high-sensitivity modulation formats and proper dimensioning of optical antennas. The trade-off may depend on different performance parameters, as well as engineering choices.

As said, in the following, we will assume that the transmitter (TX) and the receiver (RX) are optimally aligned and that the received light is directly coupled into an optical fiber: this is a very effective means to detect high-speed signals, because they can be hardly received using free-space bulky receivers (high-bandwidth photodiodes have small sizes and typically come with fiber pigtails). However, fiber coupling introduces a (limited) loss of around 3 dB.

To design the link, we then selected three system options that are described in the following and whose main features are summarized in Table 1. In all cases, we assume the use of a common forward error correction (FEC), able to correct errors with high efficiency [22]; thus all the values reported in Table 1 refer to the target pre-FEC bit error ratio (BER) of 10^{-3}, which is a value commonly achieved by commercial Reed Solomon implementations.

Among the three modulation formats considered, the first is optical non-return-to-zero on–off keying (NRZ-OOK): it is based on intensity modulation; thus it is the simplest format and has the simplest RX, based on a high-bandwidth photodiode (PD). Although its quantum-limited sensitivity is around 10 PPB at BER $= 10^{-3}$, in real systems NRZ-OOK is well

known to have a far poorer sensitivity (>100 PPB) whenever detected by a common PD [17]. However, we will assume that the RX includes a low-noise erbium doped fiber amplifier (EDFA), as a pre-amplifier; in this case, it is well known that the system performance is set by the optical signal to noise ratio (OSNR) at the EDFA output; as the EDFA is operated in the small-signal regime, the OSNR is determined by the signal power (P_{in}) at the input of the pre-amplifier [17]: from there, we derive a PPB sensitivity for a pre-amplified RX. This is much better than for a single PD, although a bit higher than the quantum limit. This value is practically independent on the chosen PD, because the system performance is practically determined by the optical noise in this regime [17].

We used numerical simulations to estimate the pre-FEC BER value as a function of OSNR. Those are not detailed for simplicity; however, they show that an optimized optically pre-amplified NRZ-OOK RX, with a narrow optical filter at the EDFA output, requires a minimum OSNR (defined over the 0.1 nm bandwidth typical of fiber communications [17]) of around 8.4 dB at 10 Gbit/s, which gives the pre-FEC BER value of 10^{-3}. Thus, if we assume that the pre-amplifier EDFA has the realistic 4 dB noise figure, the above OSNR value is obtained at around −45.5 dBm input power. The above input power can be easily converted to 22 PPB value, as reported in Table 1.

As the second option, we consider the NRZ differential phase shift keying (DPSK): it is a well-studied format that can require a Mach–Zehnder modulator at the TX and a Mach–Zehnder delay interferometer (MZDI) and balanced detection at the RX. Again, in this case, we assume a pre-amplified RX: here, the intrinsic features of DPSK, allow the target performance to be attained at a lower optical signal to noise ratio, i.e., at around 3 dB lower received power (OSNR = 5.5 dB, $P_{in} = -48.5$ dBm) than in OOK [23]. Therefore, the required PPB value would be around 11.1 PPB. We note that the implementation issues of DPSK would be quite like OOK: all components are commercially available and depend on mature industrial processes.

Finally, we selected pulse position modulation (PPM). M-ary pulse position modulation (PPM-M) was proposed and is carefully considered for photon-starved links thanks to the fact that it has the best photon efficiency [9,24]. As side effects, the signal spectral width is much larger; thus the required components (e.g., photodetectors) should have much wider bands than in OOK or DPSK at the same bit rate. Moreover, both TX and RX of PPM shall implement a specific electronic processing to convert a binary data stream to/from a PPM signal. In the following, we will thus make an assumption of PPM-16, which represents a good compromise between hardware complexity and sensitivity.

Table 1. PPB and Corresponding Input Power P_{in} of the Three Modulation Formats to Reach the Pre-FEC BER of 10^{-3}

Format	PPB	P_{in} (dBm) at 10 Gb/s	Comments and References
OOK	22	−45.5	Pre-amplified, NRZ format [23]
DPSK	11	−48.5	Pre-amplified, NRZ-DPSK with MZDI detection [23]
PPM-16	7.0	−50.4	Pre-amplified, PPM-16 [30]

The PPM RX is a critical issue: in order to achieve the best performance, PDs made of superconducting nanowires were specifically developed [25,26], where the only relevant noise source is shot noise [17]. This detector must be cooled down to enable superconductivity, and a light signal is conveyed on it by an optical fiber, so that the light coupling issue is still present. Furthermore, deadtimes prevented their use at Gbit/s rates [27,28]. Although recent improvements allowed for higher operation rates [29], there is not yet proof that this RX could be scaled up operate at 10 Gbit/s rates. For all these reasons, we will consider an optically pre-amplified RX with a conventional PD also for PPM.

We recall that in all cases the RX should have an optical filter after the pre-amplifier EDFA, to reduce the ASE-ASE beating noise [17]. The chosen filter bandwidth should be around 30 GHz, for OOK and DPSK, but much higher for PPM-16 (around 120 GHz). Furthermore, we note that in the working time window, the Doppler shift is up to around ±1.3 GHz, so that the filter width provides a tolerance wide enough and the effect of Doppler can be neglected.

Let us further discuss the specific case of PPM: here, we see that 7 PPB is the measured value for PPM-16 [30]. This figure gives a benefit of around 2 dB compared to DPSK: this is indeed consistent with the higher sensitivity of PPM-M [9], which makes PPP-M frequently proposed for space links, at low speed and with huge loss [9]. The higher the value of M, the higher the sensitivity of PPM-M [9].

However, this advantage is achieved thanks to the much lower spectral efficiency and the high complexity in coding/decoding. Both these features will have a major impact in the implementation at Gbit/s speeds: the poor spectral efficiency requires modulators, electronics, and photodiodes with higher bandwidth (around 40 GHz for PPM-16 at 10 Gbit/s) than OOK or DPSK. In addition, the TX and RX electronics must implement sophisticated electronic processing [29], which can be very challenging at 10 Gbit/s and beyond. At these speed values, the practical issues become much harder when large M values ($M \geq 32$) are considered; on the other side, low-order PPMs (e.g., PPM-4 and PPM-8) would have minor implementation issues, but they give quite limited improvements in the required OSNR (PPB) values from DPSK [9,31]. Therefore, PPM-16 was assumed to be a good compromise option between sensitivity and implementation issues, as in [30].

We also note that the OSNR values reported in Table 1 are realistic: they are confirmed by experimental measurements of the OSNR tolerance of the various formats (references given in the fourth column). In fiber links with optical amplifiers, it is well known that any given combination of bit rate and modulation format has a minimum required OSNR value, which is routinely measured [23].

In our OWC link, we have two amplifiers. The booster amplifier is saturated and thus gives no significant noise contribution; on the other hand the OWC loss is huge. Therefore the OSNR at the pre-amplifier output is simply proportional to the optical power at pre-amplifier input, hence to the input

PPB value (see last column in Table 1). Actually, the PPB values of NRZ and DPSK were derived from the data of OSNR tolerance given in [23], while the PPB of PPM-16 was derived from the measurements reported in [30]. Finally, while the required OSNR values scale with the bit rate, it is well known that the PPB values do not change when increasing the bit rate, e.g., to 40 Gbit/s: this is attained, of course, provided that the RX is consistently realized (e.g., it is not affected by hardware limitations, such as a suboptimal bandwidth of the electro-optic components).

B. Losses

As the signal to/from a GEO does not travel through the Earth atmosphere, the optical power at the RX (P_{RX}) at given distance (L) can be calculated by the well-known equation that accounts for the beam diffraction and the other sources of loss. Namely, P_{RX} is given by

$$P_{\mathrm{RX}} = P_{\mathrm{TX}} L_{\mathrm{TX}} G_{\mathrm{TX}} L_{\mathrm{OWC}} G_{\mathrm{RX}} L_{\mathrm{pe}} L_f L_{\mathrm{RX}}, \tag{1}$$

where P_{TX} is the TX output power, G_{TX} and G_{RX} are the antenna gain of the TX and of the RX telescope given by $G_{\mathrm{TX}} = (\pi D_{\mathrm{TX}}/\lambda)^2 g_T$ and $G_{\mathrm{RX}} = (\pi D_{\mathrm{RX}}/\lambda)^2$, where D_{TX} and D_{TX} are the telescope diameters at TX and RX, respectively, $g_T = 0.81$ is the telescope truncation factor [32,33], $L_{\mathrm{OWC}} = (\lambda/4\pi L)^2$ is the propagation loss, $L_{\mathrm{pe}} = \exp(-2v_{\mathrm{pe}}^2/\vartheta_d^2)$ is the loss due to the pointing error ϑ_{pe}(PE), $\vartheta_d(D_{\mathrm{TX}})$ is the beam divergence angle, and L_{fc} is the loss due to the fiber coupling at the RX.

Therefore, Eq. (1) can be rewritten as

$$P_{\mathrm{RX}} = P_{\mathrm{TX}} L_{\mathrm{TX}} \left(\frac{\pi D_{\mathrm{TX}}}{\lambda}\right)^2 g_T \left(\frac{\lambda}{4\pi L}\right)^2 \exp\left(-2\frac{\vartheta_{\mathrm{pe}}^2}{\vartheta_d^2}\right) \times L_{\mathrm{fc}} \left(\frac{\pi D_{\mathrm{RX}}}{\lambda}\right)^2 L_{\mathrm{RX}}. \tag{2}$$

We note that various contributions in Eq. (2) depend on the initial beam waist ω_0, which is set to $\omega_0 = D_{TX}/(2\alpha)$, where α is the optimal truncation factor ($\alpha \cong 1.21$); hence they depend on D_{TX} [32].

Furthermore, L_{TX} and L_{RX} indicate the optical losses of the telescopes at TX and RX sides, respectively (typical assumed value is $L_{\mathrm{TX}} + L_{\mathrm{RX}} = 6$ dB) [16]. In all the following analyses, we do not consider obscuration of the telescopes [33], which strictly depends on the specific implementation and that has only a very limited impact on the overall link budgets computation.

These above assumptions eventually allow P_{RX} to be estimated as a function of D_{TX} and D_{TX}, which determine G_{TX} and G_{RX}, respectively. Clearly, the size values of the TX and RX telescopes set another relevant practical limit. As an example, we cannot expect to host a telescope with diameter larger than 1 m on a satellite, because of practical issues. This is also a strong constraint for a transmitting/receiving station on the Moon, where a sophisticated telescope would have to be transferred, mounted, operated, and maintained.

Using the above equations, in a future GEO–Moon link we can thus estimate a significant loss between the TX and RX.

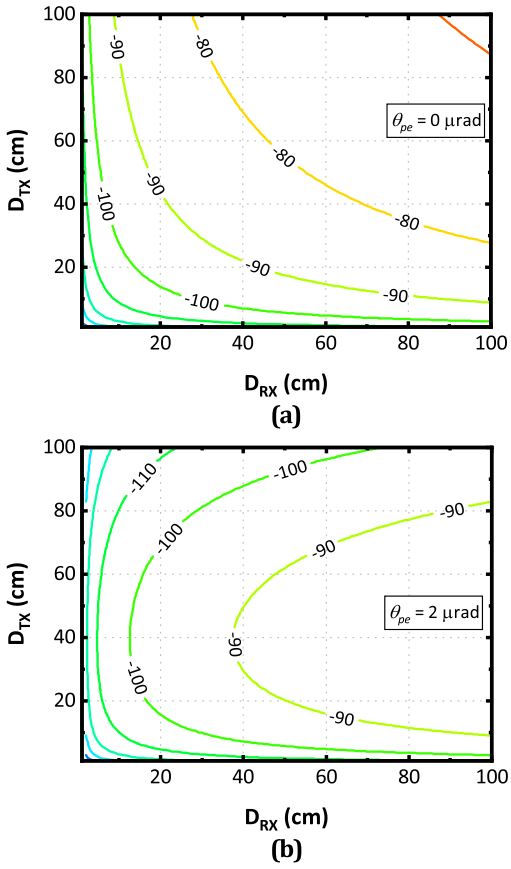

Fig. 2. Link loss (in dB) as a function of the telescope diameter of the TX and the RX at 1550 nm: (a) without pointing errors, (b) with pointing error.

The most relevant parameters affecting this loss are D_{RX} and D_{TX}. This can be seen in Fig. 2, where we report the contour plot of the loss (in dB) as a function of these two diameter values, assuming the 1550 nm wavelength (negligible changes are observed if the wavelength is 1530 or 1565 nm, extreme values of the C-band). In Fig. 2(a), we show the geometrical loss, i.e., the loss assuming perfectly aligned telescopes ($L_p = 0$ dB). We see that if we have two medium-sized OWC telescopes with 20 cm diameter, the overall loss of power is around 100 dB, which is a very high value.

We outline that, as an example, in the above figure we neglected the pointing error (PE); however, this is a well-known unavoidable effect, mostly due to external vibrations [34–36].

Although specific mechanical stabilizations can be adopted to strongly reduce them, PEs are well known to set a fundamental limit to practical OW communications. In carefully optimized systems, an excellent ϑ_{pe} value of 2 μrad ($= 3\sigma$) is expected. As indicated above, this ϑ_{pe} value produces an effect that depends on the asymptotic divergence of the light beam: the lower the divergence, the higher the effect of the PE. Indeed, this limits strongly the freedom to choose the TX telescope diameter: when considering only geometrical loss, we could propose to use huge telescopes, i.e., narrow beams, which would give higher intensity at the RX. However, the impact of pointing errors increases strongly with narrow beams

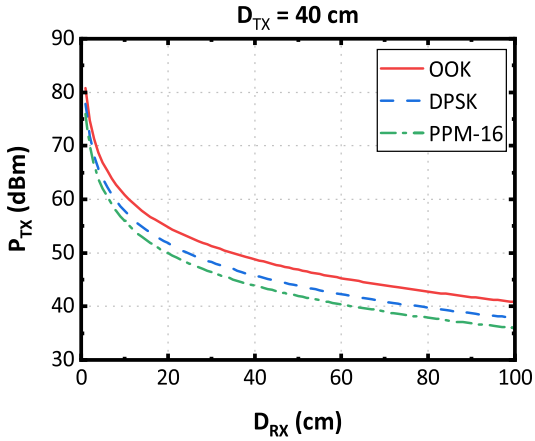

Fig. 3. Required TX optical power versus telescope diameters, assuming that the TX size is optimized to 40 cm, according to Fig. 2(b).

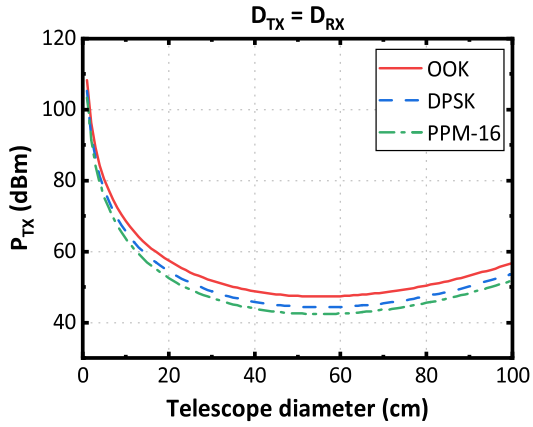

Fig. 4. Required TX optical power versus telescope diameters, assuming that both TX and RX telescopes have the same size (DRX = DTX). Pointing errors dominate when the telescope diameter is larger than 60 cm.

[34] Thus, if we include this effect, a different estimation of the practical loss is obtained, as we report in Fig. 2(b). As expected, the most notable effect of the pointing error is that the total loss is not monotonically decreasing when increasing the D_{TX} value. Indeed, increasing the beam waist, we obtain a lower divergence: in principle this allows for higher intensity at the RX, but it makes the whole system by far more sensitive to PEs. On the other hand, we highlight that, as known, the pointing error is not much affected by the RX diameter (the received beam width is typically much larger than D_{RX}).

Indeed, unlike what we obtained for the TX, when increasing the size of the telescope at RX, we obtain a monotonic improvement of RX power. These results are reported in Fig. 3. Here, we present the minimum required P_{TX} for an optimized TX telescope, with $D_{TX} = 40$ cm, as derived from Fig. 2(b). For comparison, in Fig. 4 we report the corresponding results taken for the symmetric case $D_{TX} = D_{RX}$. As a result of this optimization, we see that the required power values, for all three formats, can be quite lower than in the previous case, and they can be further reduced by very large communication telescopes.

While astronomical telescopes are quite large, today, a 1 m telescope seems to be the largest one that we can consider for communication applications. Indeed, large OWC telescopes have some major practical issues: they are more difficult to be realized and have stronger issues related to stability and maintenance. We can therefore expect that the maximum size of these telescopes would be 1 m. Assuming this value, comparing Figs. 3 and 4, we observe an improvement of around 5 dB in the power budget for each format if we fix $D_{TX} = 40$ cm and then optimize D_{RX}.

3. RESULTS

A. 10 Gbit/s Link

As a consequence of Figs. 3 and 4, we see that two alternative system architectures can be envisaged to design and realize a bidirectional optical GEO–Moon link. As the first option, we can adopt a single telescope with the same diameter for TX and RX, at both ends ($D_{TX} = D_{RX}$). Thus, the same telescope would transmit and receive optical wireless signals, simultaneously. This option is clearly the most compact and could allow for simple solutions: indeed, it can exploit the same optics for the two transmission directions.

On the other side, we can also foresee a second option, i.e., having two separate telescopes for transmitting and receiving at each end of the link. This can offer a significant optimization, although it would be more demanding in terms of optics, then also in terms of required space and weight. However, the key benefit of this second approach is that it can result in a large reduction of P_{TX} power, thus decreasing the requirement of power supply and EDFA output power. Equivalently, this degree of freedom can be used to provide higher data rates at fixed output power.

To this aim, we note that at the signal wavelength of 1550 nm, the highest power reachable by an optical (fiber) amplifier is obtained by erbium–ytterbium doped fibers [37]. For these amplifiers, the output saturation power is today not higher than 43 dBm [38]. Although higher power values might be achieved in the future, this seems a consolidated value for such an extreme environment as the Moon and, to lower extent, the GEO satellite.

Therefore, we then fix $P_{TX} = 43$ dBm, and we can then estimate the corresponding P_{RX}. Clearly, because of the practical limitations of P_{TX}, the second system option, i.e., different telescope sizes, is preferrable for high-speed data.

Thus, if we fix the D_{RX} value to be 1 m, we can then calculate the PPB values that could be achieved at 10 Gbit/s, for different D_{TX} values and variable P_{TX} values: these are presented in Fig. 5, where we explicitly indicate the contour levels corresponding to the PPB values given in Table 1 for the three formats. We also highlight the limiting value of 43 dBm TX power (dashed black vertical line). As can be seen, when limiting the optical power, the OOK format can successfully operate over a very small region. Namely, it would require a large telescope at RX and quite different sizes of telescopes (the best combination would be 40 cm at TX and 100 cm at RX). Clearly, the different modulation formats can provide different margins having different PPB values at pre-FEC level. Alternatively, they give a different level of flexibility in the

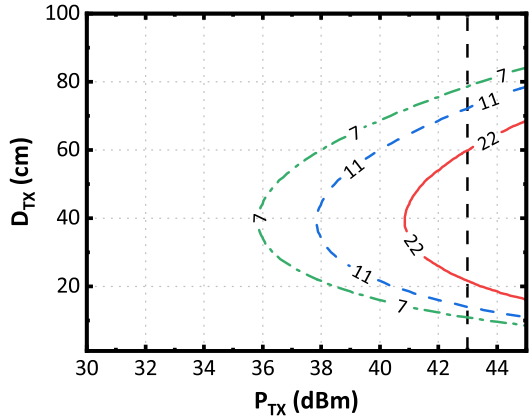

Fig. 5. PPB values at the RX, for 10 Gbit/s signals, when assuming a RX telescope with 1 m diameter (labels indicate the minimum PPB values for the three modulation formats). The value of the maximum P_{TX} (43 dBm) is indicated by the dashed vertical line.

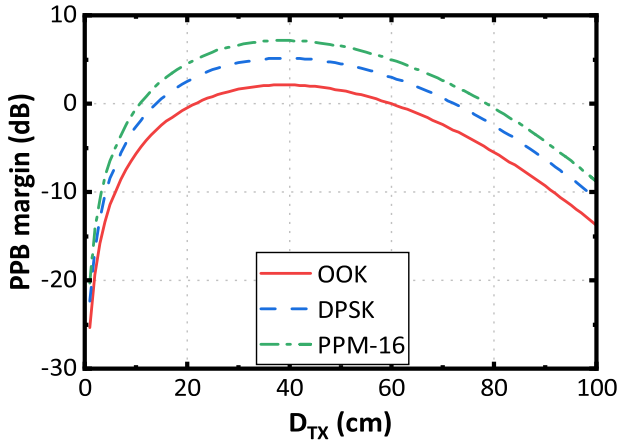

Fig. 6. System margin of 10 Gbit/s signals for the three formats. We assume a RX telescope with 1 m diameter and exactly the maximum TX power ($P_{TX} = 43$ dBm).

choice of the D_{TX} value: as an example, in Fig. 6, we report the calculated system margin values for the three formats fixing $D_{RX} = 1$ m at RX and exactly $P_{TX} = 43$ dBm. As we see, for OOK a very limited range of D_{TX} values can allow an effective link to be realized, i.e., those values giving a positive margin. In particular, a minimum D_{TX} value of around 22 cm is required. DPSK has a wider operational range than OOK. PPM-16 can have even lower D_{TX} values, although the improvement from DPSK is not very high.

We can also try to design the link assuming symmetric telescopes (i.e., assuming $D_{TX} = D_{RX}$); in that case, we expect that the OOK format cannot work, based on the results showed in Fig. 4.

This is indeed confirmed by our calculations, which are not reported explicitly here: they indeed show that a symmetric link cannot work for the other two formats either. In the symmetric configuration, none of the three modulation formats can reach the minimum power level required for the effective transmission. The symmetric configuration should then be considered only for signals at lower rates.

The above conclusion about symmetric telescopes is determined by various elements, namely, the PPB sensitivity values, which is a feature of the modulation format, the optical loss, and the maximum TX power. Both telescope sizes have a relevant impact on the loss, as one can expect from diffraction theory (or equivalent antenna gain for the telescopes). Without PE, the impact of two diameters is the same. However, when the impact of PE cannot be neglected, the role of the two telescopes is quite different: this is a consequence of the fact that L_{pe} loss depends on the beam divergence, which is proportional to the inverse of the TX diameter. In this case, the role of the two telescopes becomes asymmetric, because only the TX diameter affects the PE (as shown in [34]).

Therefore, when we consider PE, we should prefer a smaller TX telescope, as it has slightly wider divergence: this can effectively mitigate the impact of the PE. On the other hand, this leads to a lower received intensity. Hence, in order to compensate for that and to increase the collected power, we should then prefer a slightly wider RX telescope.

Unfortunately, if we want to use symmetric telescopes, the chosen limit of transmitter power is not high enough for any of the considered formats at 10 Gbit/s. Indeed, this configuration lacks the flexibility of an additional degree of freedom, which strongly limits the power budget. In that configuration, the only solution would be to introduce significant modifications of our basic assumptions: these can involve much stronger FEC codes and/or a booster amplifier having much higher power than what we assumed so far.

4. FUTURE UPGRADES

After 10 Gbit/s links will be realized, we will likely need to scale up the total capacity. Thus, it is important to estimate the opportunities of future upgrades for the different modulation formats.

As we have seen that 10 Gbit/s links already imply asymmetric systems, we performed the analysis assuming this last configuration only. The obtained results are presented in Fig. 7, where we report the level curves corresponding to the minimum achievable capacity for the three modulation formats, i.e., OOK, DPSK, and PPM-16 from top to bottom. We present here the level curves corresponding to different bit rate values, including 20 and 40 Gbit/s. For the sake of completeness, we include also capacity values lower than 10 Gbit/s.

From the reported results, we can see that the OOK format cannot be upgraded to 20 Gbit/s, as indeed we had a quite small operating region even at 10 Gbit/s. The DPSK format, on the other side, has clearly a potential to be upgradable to 20 Gbit/s and even to 40 Gbit/s. A similar condition is observed for PPM-16. In both last cases, the 40 Gbit/s working region is, however, quite limited: as a result, under current assumptions, we cannot expect to reach the 80 Gbit/s capacity. To this aim, we should indeed include the deployment of amplifiers with higher output power (greater than 46 dBm, at least), or assume even wider telescopes.

Finally, we expect that speed values higher than 40 Gbit/s can be hardly achieved, unless new optical technologies could be introduced.

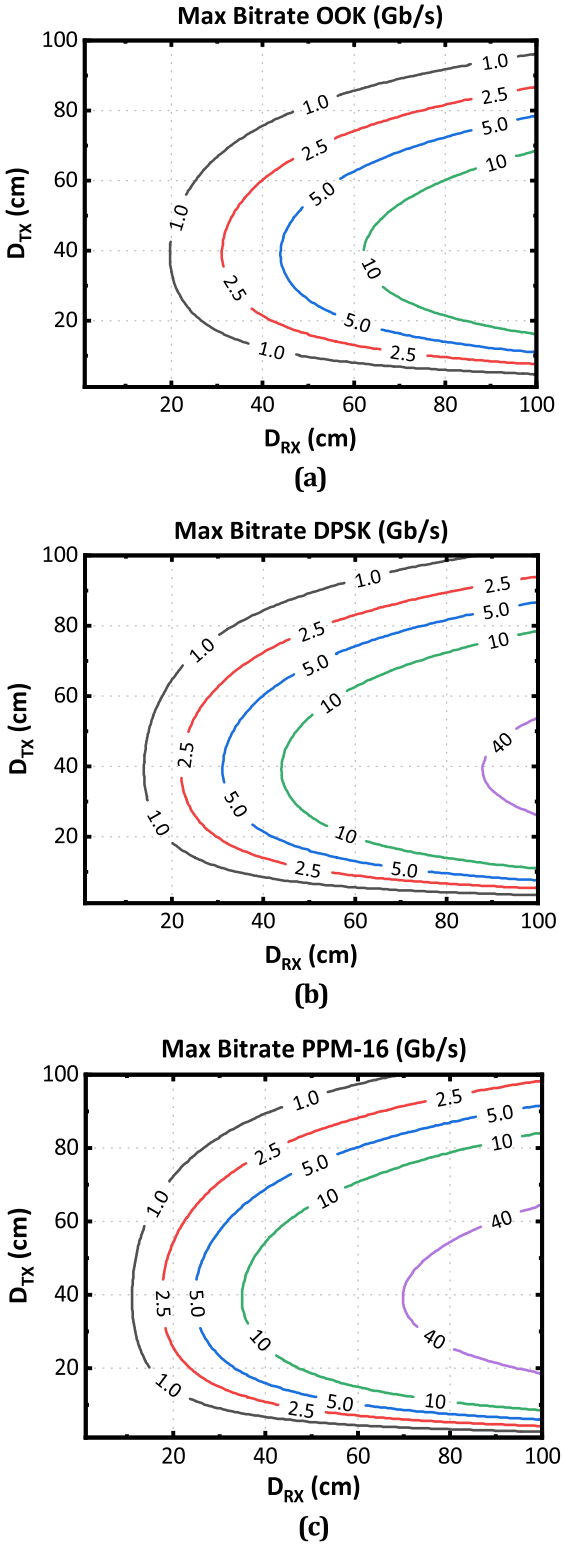

Fig. 7. Level curves indicating the maximum bit rate (labels, in Gbit/s) attainable at maximum power $P_{TX} = 43$ dBm, and different TX and RX telescope diameter values, for the three modulation formats.

5. CONCLUSION

By means of a comprehensive analysis, we demonstrated for the first time that a 10 Gbit/s wireless link connecting Earth to the Moon can be realized by using existing fiber communication technologies combined with optimized, yet realistic, telescopes and common FEC. We proposed that the link be established by means of a GEO satellite orbiting around Earth. One of the most relevant issues over the considered propagation distance is due to beam spreading, intrinsic in the wave nature of light. This strongly limits the received intensity, and thus the final received photon/bit values. Our analysis also showed that another key limitation is the residual pointing error, which has a strong impact on the choice of TX beam width. This last effect makes strongly preferable a system where the TX and RX telescope sizes are different.

We have thus derived a practical size of telescopes that could be realistically used to transmit and collect the signal, and then combined the propagation features with the sensitivity of the most likely choices for modulation format and signal detection. We saw that current optical fiber communication technology can be exploited to realize 10 Gbit/s GEO-to-Moon links. It could also be used to upgrade to 40 Gbit/s transmission, although with lower margins and tolerances: in that case, specific space-graded transceivers suitable for high-sensitivity formats (e.g., DPSK or PPM-16) should be developed, based on existing devices. This can be possible thanks to the intrinsic feature of a lower PPB value required by DPSK or PPM (see Table 1).

Finally, we would like to outline a significant difference in the implementation of DPSK and PPM formats. While a DPSK RX could be realized using existing technology, a 10 Gbit/s PPM RX will need a dedicated development, due to the intrinsic complexity of its hardware architecture; indeed PPM requires modulators, drivers, and detectors with much higher bandwidth than OOK (or DPSK) at the same bit rate, e.g., around 40 GHz for a 10 Gbit/s PPM-16. Furthermore, the electronics of any PPM RX should realize complex functionalities (as shown in [30]): those can be demonstrated in the lab, e.g., by offline processing, but they still require a significant effort to be integrated into a commercial chipset.

Moreover, in a future upgrade to 40 Gbit/s, PPM-16 would need modulators, electronic amplifiers, and detectors with around 160 GHz bandwidth. Also, the electronic processing should be scaled accordingly. This can have a non-negligible impact on deployment times.

Funding. This work was partly supported by the European Space Agency and Agenzia Spaziale Italiana under the contract "Optical Communications Requirements for Scientific Missions and the Deep Space Gateway" (Contract 1550007214).

Disclosures. The authors declare no conflicts of interest.

REFERENCES

1. M. Smith, D. Craig, N. Herrmann, *et al.*, "The Artemis program: an overview of NASA's activities to return humans to the Moon," in *IEEE Aerospace Conference* (2020).
2. A. Witze, "Lift off! Artemis Moon rocket launch kicks off new era of human exploration," Nature **611**, 643–644 (2022).
3. X. Lin, Z. Yongliao, and J. Yingzhuo, "China's planning for deep space exploration and lunar exploration before 2030," Chin. J. Space Sci. **38**, 591–592 (2018).
4. R. M. Smith, N. Merancy, and J. Krezel, "Exploration missions 1, 2, and beyond: first steps toward a sustainable human presence at the Moon," in *IEEE Aerospace Conference* (2019).

5. H. K. Athanasopoulos, "The Moon Village and space 4.0: the 'Open Concept' as a new way of doing space?" Space Policy **49**, 101323 (2019).
6. J. Woerner and B. Foing, "The "Moon Village" concept and initiative," in *Annual Meeting of the Lunar Exploration Analysis Group* (2016).
7. D. P. Karanam, M. Bhatt, S. Sathyan, *et al.*, "Contextual characterisation study of Chandrayaan-3 primary landing site," Mon. Not. R. Astron. Soc. Lett. **526**, L116–L123 (2023).
8. Y. Sugito, S. Iwasaki, K. Chida, *et al.*, "A study on the required video bit-rate for 8K 120-Hz HEVC/H.265 temporal scalable coding," in *Picture Coding Symposium (PCS)* (2018), pp. 106–110.
9. H. Hemmati, ed., *Deep Space Optical Communications* (Wiley, 2006).
10. L. J. Deutsch, "Towards deep space optical communications," Nat. Astron. **4**, 907 (2020).
11. J. D. Moores and K. E. Wilson, "The architecture of the laser communications relay demonstration ground stations: an overview," Proc. SPIE **8610**, 86100L (2013).
12. D. M. Boroson, B. S. Robinson, D. V. Murphy, *et al.*, "Overview and results of the Lunar laser communication demonstration," Proc. SPIE **8971**, 89710S (2014).
13. H. Ivanov, Z. Hatab, and E. Leitgeb, "Channel emulation of satellite-to-ground APD-based OWC link in the presence of atmospheric turbulence fading," in *16th International Conference on Telecommunications (ConTEL)* (2021), pp. 33–36.
14. I. Toselli, L. C. Andrews, R. L. Phillips, *et al.*, "Free space optical system performance for a Gaussian beam propagating through non-Kolmogorov weak turbulence," IEEE Trans. Antennas Propag. **57**, 1783–1788 (2009).
15. M. Toyoshima, S. Yamakawa, T. Yamawaki, *et al.*, "Long-term statistics of laser beam propagation in an optical ground-to-geostationary satellite communications link," IEEE Trans. Antennas Propag. **53**, 842–850 (2005).
16. T. Araki, "A trade-off study of Lunar-earth optical communication links," Proc. SPIE **11852**, 118521X (2021).
17. G. P. Agrawal, *Fiber-Optic Communication Systems*, 5th ed. (Wiley, 2021).
18. Y. Arimoto, "Compact free-space optical terminal for multi-gigabit signal transmissions with a single-mode fiber," Proc. SPIE **7199**, 719908 (2009).
19. E. Ciaramella, Y. Arimoto, G. Contestabile, *et al.*, "1.28 terabit/s (32×40 Gbit/s) WDM transmission system for free space optical communications," IEEE J. Sel. Areas Commun. **27**, 1639–1645 (2009).
20. J. W. Alexander, S. Lee, and C.-C. Chen, "Pointing and tracking concepts for deep-space missions," Proc. SPIE **3615**, 230–249 (1999).
21. D. Divsalar, M. S. Net, and K.-M. Cheung, "Acquisition and tracking for communications between Lunar South Pole and Earth," in *IEEE Aerospace Conference*, Big Sky, Montana, 2019.
22. T. Afxendios, O. Koufopavlou, and I. Tomkos, "FEC in optical communications," IEEE Circuits Devices Mag. **22**(6), 79–86 (2006).
23. A. H. Gnauck and P. J. Winzer, "Optical phase-shift-keyed transmission," J. Lightwave Technol. **23**, 115–130 (2005).
24. G. Cancellieri, "Transmission efficiency in photon counting channels," IEEE Trans. Commun. **37**, 183–187 (1989).
25. M. E. Grein, A. J. Kerman, E. A. Dauler, *et al.*, "An optical receiver for the Lunar Laser Communication Demonstration based on photon-counting superconducting nanowires," Proc. SPIE **9492**, 949208 (2015).
26. H. Ivanov, E. Leitgeb, P. Pezzei, *et al.*, "Experimental characterization of SNSPD receiver technology for deep space OWC under laboratory testbed conditions," Optik **195**, 163101 (2019).
27. B. S. Robinson, A. J. Kerman, E. A. Dauler, *et al.*, "781 Mbit/s photon-counting optical communications using a superconducting nanowire detector," Opt. Lett. **31**, 444–446 (2006).
28. M. M. Willis, A. J. Kerman, M. E. Grein, *et al.*, "Performance of a multimode photon-counting optical receiver for the NASA Lunar Laser Communications Demonstration," in *International Conference on Space Optical Systems and Applications (ICSOS)* (2012).
29. B. S. Robinson, A. J. Kerman, E. A. Dauler, *et al.*, "Demonstration of gigabit-per-second and higher data rates at extremely high efficiency using superconducting nanowire single photon detectors," Proc. SPIE **6709**, 299–306 (2007).
30. N. W. Spellmeyer, S. L. Bernstein, D. M. Boroson, *et al.*, "Demonstration of multi-rate thresholded preamplified 16-ary pulse-position-modulation," in *Optical Fiber Communication Conference (OFC)* (2010), paper OThT5.
31. S. Hamid, "Performance evaluation of optically pre-amplified M-ary PPM systems for free-space optical communications," Master's thesis (American University of Sharjah, 2012).
32. B. J. Klein and J. J. Degnan, "Optical antenna gain. 1: transmitting antennas," Appl. Opt. **13**, 2134–2141 (1974).
33. R. N. Wilson, *Reflecting Telescope Optics II: Manufacture, Testing, Alignment, Modern Techniques* (Springer, 2013).
34. H. Hemmati, ed., *Near-Earth Laser Communications*, 2nd ed. (CRC Press, 2020).
35. C.-C. Chen and C. S. Gardner, "Impact of random pointing and tracking errors on the design of coherent and incoherent optical intersatellite communication links," IEEE Trans. Commun. **37**, 252–260 (1989).
36. S. Arnon and N. S. Kopeika, "Laser satellite communication network-vibration effect and possible solutions," Proc. IEEE **85**, 1646–1661 (1997).
37. M. Storm, D. Engin, B. Mathason, *et al.*, "Space-based erbium-doped fiber amplifier transmitters for coherent, ranging, 3D-imaging, altimetry, topology, and carbon dioxide lidar and earth and planetary optical laser communications," EPJ Web Conf. **119**, 02002 (2016).
38. "Amonics AEDFA-43-R datasheet," https://www.amonics.com.hk/view?path=/amonics/datasheets/11/datasheet.pdf.

Ernesto Ciaramella (Senior Member, IEEE) joined as an Associate Professor Scuola Superiore Sant'Anna, Pisa, in 2002, where he has been a Full Professor of telecommunications with Istituto TeCIP since 2014. He is the author or coauthor of about 250 publications and holds 25 international patents. He participated in several European research projects. He was coordinator of the EU-FP7 Project COCONUT from 2012 to 2015. He is currently the principal investigator of the ESA–TOWS project about optical wireless systems for intra-spacecraft links. His research interest includes various topics in optical communications (components, systems, and networks). His main research contributions are related to devices for the regeneration of the optical signal, the design of WDM systems for core and access networks, and free-space optical systems (optical wireless).

Veronica Spirito, a Ph.D. student at Scuola Superiore Sant'Anna, Pisa, is involved in research activity applied to long-haul OWC communications within various ESA research projects (e.g., HydRON). As a system engineer, she is modeling the design of an end-to-end free-space optical WDM system for satellite communications. Focusing on the physical layer and signal propagation, she has also been at DLR German Aerospace Center (Munich, Germany) to conduct theoretical analysis and field trials of Earth-satellite optical links.

Giulio Cossu received his M.S. degree in physics from the University of Pisa, Italy, in 2010. He obtained his Ph.D. degree in 2014 at Scuola Superiore Sant'Anna (SA), Pisa. Currently, he is an Assistant Professor at SA. The main topic of his thesis was the investigation of innovative solutions for optical wireless communications (OWC). His research interests include the areas of optical propagation through the atmosphere, optical characterization, and optical communication. He was the scientist responsible for SA for the projects "High Throughput Optical Network (HYDRON)" and "HYDRON Simulation TestBed," founded by European Space Agency (ESA). He was in the workgroup about the development of optical wireless links for intra/extra spacecraft and AIT scenarios within the framework of the TOWS project, funded by ESA. He is the author or co-author of about 70 publications and holds 4 international patents.